

Monosodium glutamate as a draw solute for sewage thickening by forward osmosis–nanofiltration

Seunghoon Yang^{1,2}, Taekguen Yun^{1,2}, Soon Bum Kwon^{1,2}, Kyungjin Cho¹, Seongpil Jeong¹,
Seungkwan Hong^{**2} and Seockheon Lee^{*1,2}

¹Water Cycle Research Center, Korea Institute of Science and Technology, Seoul 02792, Republic of Korea

²Advanced Environmental Science, Energy Environment Policy and Technology, KU-KIST Green School, Graduate School of Energy and Environment, Korea University, 145, Anam-ro, Seongbuk-gu, Seoul 02841, Republic of Korea

(Received January 11, 2020, Revised April 30, 2021, Accepted May 30, 2021)

Abstract. Monosodium glutamate (MSG) was evaluated as a draw solute (DS) of forward osmosis–nanofiltration (FO–NF) process for sewage thickening. Water flux (J_w) and reverse draw solute flux (J_s) through FO membrane with MSG were compared to those with NaCl as the reference DS. In addition, the influence of MSG to anaerobic digestion of concentrated sewage for methane gas production was investigated. The J_s/J_w for MSG was 0.0015 mol/L at 1M of initial concentration with a CTA(HTI) membrane, which was 6 % of that for NaCl, while the water flux (J_w) for MSG (ca. 10 L/m²h) was comparable to that for NaCl in FO processes. MSG recovered up to 98% by NF process, which changed with applied membrane and MSG concentration. The collected primary effluent from the full-scale wastewater treatment plant was thickened up to nine times in terms of volumetric concentration factor. The physical membrane flushing by a water could effectively recover the flux. The inhibitory effects of MSG on anaerobic methane production could be negligible and the gas production potential increased.

Keywords: anaerobic toxicity assay; forward osmosis; monosodium glutamate; nanofiltration; reverse solute flux; sewage thickening

1. Introduction

The severe worldwide water shortage has been raised a critical issue owing to climate changes, population growth, industrialization, and urbanization. In order to overcome the water shortage in urbanized areas, the water reuse technology has been suggested (Batstone *et al.* 2015, Jiang *et al.* 2018). However, the energy requirement for the additional treatment for water reuse in the conventional wastewater treatment plant is high. In order to overcome these problems, several recent studies have proposed the use of alternative wastewater treatment plant (AWWTP) systems, which can simultaneously produce high quality reusable water and energy (Holloway *et al.* 2007, Cath *et al.* 2006). The typical AWWTP systems use membrane separation and anaerobic digestion (AD). The membrane separation in the AWWTP system thickens feed wastewater, which can facilitate the AD operation. A highly thickened wastewater allows the use of smaller anaerobic digesters, increases the volumetric biogas (methane) production, and decreases the heating energy (Liu *et al.* 2016).

Conventional membrane processes such as nanofiltration (NF) and reverse osmosis (RO) have been applied in the AWWTP. However, these membrane

processes are faced to severe membrane fouling and required frequent membrane cleaning. In order to overcome these disadvantages, forward osmosis (FO) membrane processes have recently been suggested for thickening of wastewaters (Chen *et al.* 2014, Xue *et al.* 2015). FO uses the osmotic pressure of a highly concentrated solution with a chemical potential to draw water across a semipermeable membrane from a low-concentration solution with a low water chemical potential (Ghadiri *et al.* 2019). The FO process has several advantages including a 1) smaller fouling owing to the absence of hydraulic pressure across the membrane, 2) low energy requirement, and 3) high removal for ions.

The FO process has been applied to wastewater treatment. Chen *et al.* (2014) studied the performance of a submerged membrane bioreactor with FO separation over 22 days; the removal rates of organic carbon, NH₄⁺-N, and total phosphate (TP) reached 96, 60, and 100%, respectively. Xue *et al.* (2015) reported an FO process for a municipal wastewater treatment using seawater as the draw solute and achieved a 2.3-times-thickened wastewater.

Several previous studies have been carried out for regeneration of draw solution and water production in the FO process and hybrid processes linking the FO process. The draw solutes were classified into five types (Ge *et al.* 2013), 1) volatile compounds such as ammonium bicarbonate (McCutcheon *et al.* 2006), 2) nutrient compounds such as glucose and fructose (Kravath *et al.* 1975, Yong *et al.* 2012, Lutchmiah *et al.* 2014), 3) inorganic salts such as sodium chloride (Achilli *et al.* 2010), 4) organic salts such as sodium formate, sodium acetate, sodium propionate, and magnesium acetate (Bowden *et al.*

*Corresponding author, Professor,
E-mail: seocklee@kist.re.kr

**Co-Corresponding author, Professor,
E-mail: skhong21@korea.ac.kr

2012), and 5) synthetic materials such as hydrophilic magnetic nanoparticles (MNPs), polyelectrolytes of polyacrylic acid sodium (PAA-Na), and polymer hydrogels (Ling *et al.* 2011).

Draw solute developments for target FO applications were also reported. Ansari *et al.* (2015) investigated various applicable draw solutes for FO with AD to facilitate the resource recovery. When the FO–AD process is considered, the inorganic solutes can inhibit AD microbes, thereby decreasing the efficiency and biogas production (Kugelman *et al.* 1964, Patel *et al.* 1977, Chen *et al.* 2008).

Hau *et al.* (2014) investigated an FO–NF hybrid process using ethylenediaminetetraacetic acid (EDTA) sodium as a novel draw solute for reconcentration. Kumar *et al.* (2009) reported rejection of NaCl in an NF system using variant membranes. Ideal draw solute can provide high osmotic pressure, easy separation, low reverse salt flux, and no adverse effect to the treatment system. For the suggested AWWTP systems with FO–NF, diffused salts into the wastewater concentrate through the FO membrane can influence the following anaerobic digestion process for the methane gas production.

Non-toxicity to anaerobic digestion with low J_s/J_w ratio is important for the selection of draw solute. Commercially available food additives can be suggested as the candidates. Therefore, we investigated monosodium glutamate (MSG) as a novel draw solute in the FO-based wastewater treatment process. In order to evaluate the application feasibility of the MSG draw solute to the wastewater reuse process, tests were carried out including a 1) performance evaluations on flux, reverse salt flux (RSF), and J_s/J_w of the FO membrane process under deionized (DI) water conditions, 2) FO-based sewage thickening process including membrane cleaning using a primary effluent of the wastewater treatment plant, 3) draw solute recovery using an NF system, and 4) evaluation of the potential inhibitory effect on microbes by the draw solute in the FO–AD process.

2. Materials and methods

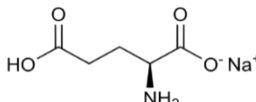
2.1 Draw solutes

MSG (Duksan, Korea) and NaCl (Daesang, Korea) solutes were purchased. The characteristics of each draw solute are presented in Table 1. NaCl was used as a reference draw solute. The molecular weight and diffusion coefficient of MSG are 2.8 and 0.56 times those of NaCl, respectively. The MSG molecule is significantly larger, heavier, and more complex than the NaCl molecule.

2.2 Membrane

Flat sheet-type cellulose triacetate (CTA) membrane (Hydration Technology Innovations (HTI), Albany, OR) and lab fabricated mLBL membrane (Kwon *et al.* 2015) were used for FO processes. For draw solute recovery, NF membranes were tested. The characteristics of the NF membrane is shown in Table 2.

Table 1 Characteristics of the tested draw solutes

Draw solute	Molecular weight (g/mol)	Diffusion coefficient D (10^{-9} m ² /s)	Chemical structure
Sodium chloride	58.44	1.49 (0.9 mol/L)*	Na - Cl
MSG	169.11	0.84 (0.1 mol/L)**	

*Achilli *et al.* 2009, **Ribeiro *et al.* 2014

Table 2 NF membrane characteristics

Membrane	MWCO(Da)	Salt rejection (%)		
		NaCl	MgSO ₄	CaCl ₂
NE4040-90 (Toray Chemical Korea)	210 ¹⁾	85–95 ²⁾	97 ²⁾	90–95 ²⁾
NF4040(Dow Filmtec)	-	-	98 ^{>2)}	-

¹⁾ From published data (Lee *et al.* 2008)

²⁾ From manufacturer's product catalog

Table 3 Characteristics of the sewage used in this study

Sample	TCOD* (mg/L)	SCOD** (mg/L)	T-N*** (mg/L)	Ammonia (mg/L)	T-P**** (mg/L)
Sewage	271	142.5	30.9	32.4	2.9

*TCOD: Total COD, **SCOD: Soluble COD, ***T-N: Total Nitrogen, ****T-P: Total Phosphorus

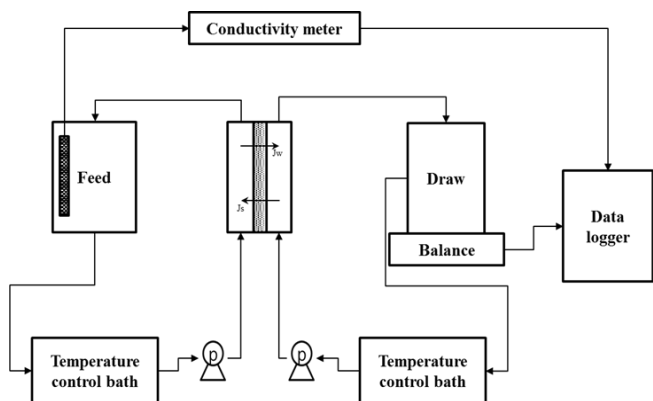


Fig. 1 Schematic diagram of the FO process used in this study

2.3 Experimental conditions for membrane processes

DI water and sewage (primary wastewater) were used as feed solutions for the FO performance tests and sewage thickening by the FO process. The sewage characteristics are shown in Table 3. The membrane was physically flushed using DI water at 1 L/min through both feed and draw sides for 5 min for performance recovery.

Fig. 1 shows a schematic diagram of the FO experimental setup. The flow direction across the membrane was co-current. The temperatures of the feed and draw solutions were maintained at 25°C using a temperature control bath.

The experimental conditions in the FO experiments are shown in Table 4. An FO membrane can be used in two

Table 4 Feed and draw side experimental conditions for the MSG performance test and sewage thickening

Experiment (tested membrane)	Feed side		Draw side	
			Concentration	
FO performance tests (CTA membrane)	DI water	MSG solution	0 – 3 M	
(mLBL membrane)	DI water	MSG solution	0 – 3 M	
Sewage thickening (CTA membrane)	Sewage*	MSG solution	1 M	

*DI water was loaded for blank run

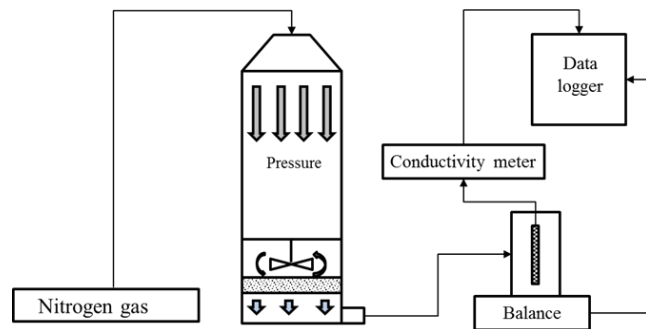


Fig. 2 Schematic diagram of the NF process for DS recovery

driving modes, where the active layer faces the feed solution (AL–FS mode) and the support layer faces the feed solution (SL–FS mode). The performances of FO processes using NaCl and MSG were compared and evaluated based on the water flux (J_w), RSF(J_s), and J_s/J_w ratio.

J_w was calculated with the following equations.

$$J_w = \frac{\Delta V}{A_m \Delta t} \quad (1)$$

$$J_s = \frac{\Delta CV}{A_m \Delta t} \quad (2)$$

where ΔV is the volume change of the draw solution, ΔCV is the permeated salt to feed solution, A_m is the effective membrane area and Δt is the interval time. Experiment was conducted three times for each concentration to obtain an average value. In each experiment, a new membrane was used to minimize the fouling by draw solute. However, in the sewage thickening experiment, the same membrane was used to confirm the effect of cleaning. In the experiment to confirm the characteristics of MSG as a draw salt, the average water and solute flux was calculated for 100 ml of permeated water volume. In sewage thickening experiment, the flux was measured with 50 ml of permeated water at intervals in order to observe the change in water flux during the progress of thickening.

Fig. 2 shows a schematic diagram of the NF experimental setup for draw solute recovery. The initial feed solution volume of 100 mL was loaded in a custom-pressure stainless-steel vessel. The feed solution was pushed to the outside of the vessel by nitrogen at a constant pressure. The volume of collected water was 15 mL. The concentration of collected water passed through the membrane was

measured. The temperature of the feed solution was maintained at 25°C.

2.4 Anaerobic toxicity assay (ATA)

An ATA (ISO, 2003) was performed to investigate the influence of MSG on the methane production. This methodology has been widely used to assess the toxic effects of some chemicals on the methane production (Owen *et al.* 1979, Gartiser *et al.* 2007). The ATA was carried out in 125-mL serum bottles (working volume: 100 mL). Two milliliters of a stock solution containing nutrient broth (100 g/L), yeast extract (100 g/L), and D-glucose (100 g/L) were added to each serum bottle. According to the experimental conditions, 48 mL of the MSG solutions were added to each serum bottle; the final MSG concentrations were set to 0, 4.4, 15.2, 43.5, 152.2, and 239.1 mM. The anaerobic sludge collected from a full-scale mesophilic AD plant was inoculated at a ratio of 50% (v/v). The pH was adjusted to 7.0 ± 0.1 using 0.1 N NaOH. All serum bottles were purged with nitrogen gas (N_2) for 5 min, and then sealed with rubber septa and alumina caps. The ATA was performed in triplicate at 35°C and 150 r/min in a shaking incubator, until cell death (over 44 days).

After the ATA, the methane production potential, maximum methane production rate, and lag period were determined using a modified Gompertz model (Zwietering *et al.* 1990, Lay *et al.* 1998):

$$M = P \times \exp\left\{-\exp\left[\frac{R_m \times e}{P} \times (\lambda - t) + 1\right]\right\} \quad (3)$$

where P , R_m , and λ are the methane production potential, maximum methane production rate, and lag period, respectively.

2.5 Analytical methods

The permeate water flux was calculated using the increase in volume measured by the balance (CUX6200H, CAS) within the draw tank. The RSF of NaCl was calculated using the increase in electrical conductivity measured by the conductivity meter (HQ-40d, HACH) in the feed tank. The RSF of MSG was calculated using the increase in the sodium ion concentration within the feed tank, which was determined by ion chromatography (ICS-1000, DIONEX). The methane gas production was measured by gas chromatography (GC 6890N, Agilent TECH). To determine the MSG rejection by NF membrane, conductivity and TOC of permeate were measured. Freezing point osmometer was used for measurement of osmotic pressures of MSG and NaCl solutions.

3. Results and discussion

3.1 Performance of the FO process using MSG as a draw solute

Water drawing capability of MSG as a DS for FO process was evaluated and compared to NaCl as the

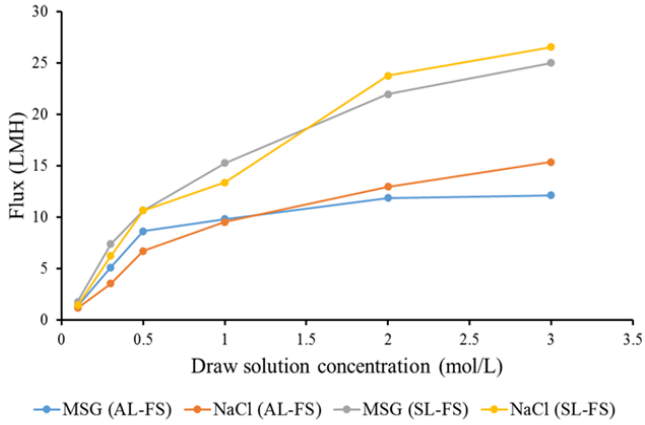


Fig. 3 Fluxes of the FO processes using MSG and NaCl as draw solutes with CTA membrane(HTI)

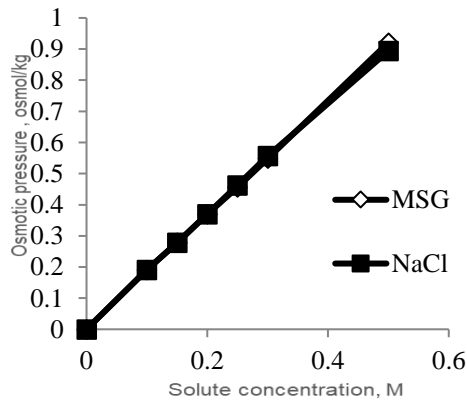


Fig. 4 Plot of molar concentration versus measured osmotic pressure of MSG and NaCl

processes with HTI CTA membrane according to the DS concentrations in the AL-FS and SL-FS modes. Water fluxes with MSG as DS were comparable to those with NaCl. In the SL-FS mode, the water flux of the FO processes using the MSG solutions with 3 M was 25.0 L/m²h. In the AL-FS mode, the water flux was about 50% lower than SL-FS mode (12.1 L/m²h). The water flux in the SL-FS mode was higher than that in the AL-FS mode as the draw solution was less diluted at the contact point on the active layer in the SL-FS mode (Cath *et al.* 2006). With the draw solution concentration increased, the water flux of the FO process exhibited a more-nonlinear (logarithmic) tendency, owing to the internal concentration polarization (ICP) and external concentration polarization (ECP), which are defined as (McCutcheon *et al.* 2006):

$$\frac{\pi_{D,S}}{\pi_D} = \exp(J_w K) = \exp(J_w S/D) \quad (4)$$

$$\frac{\pi_{D,A}}{\pi_D} = \exp(J_w/k) \quad (5)$$

where Eqs. (4) and (5) define the ICP and ECP, respectively, $\pi_{D,S}$ is the osmotic pressure of the draw solution at the contact point between the active and support layers (within

the membrane), $\pi_{D,A}$ is the osmotic pressure of the draw solution at the membrane surface (active layer), π_D is the osmotic pressure of the bulk draw solution, K is the solute resistivity for diffusion, S is the membrane structure parameter, D is the diffusivity of solute, and k is the mass transfer coefficient; $\pi_{D,A}$ and $\pi_{D,S}$ are lower than π_D . Purified water moves through the membrane from the feed to the draw solution by the effective osmotic pressure at the contact point between the active and support layers. The higher concentration of draw solute increases the water permeation through the membrane. However, the increased water permeation will contribute the dilutive concentration polarization at the active layer, which explains the diminished increase of water flux with increased osmotic pressure.

The water flux with MSG as DS was slightly lower than that with NaCl. Water flux without concentration polarization will be expected proportional to the osmotic pressure of applied draw solution. The theoretical osmotic pressure in dilute solution is defined as (law of van't Hoff):

$$\pi = iM_{solute}RT \quad (6)$$

where π is the osmotic pressure, i is the dimensionless van 't Hoff index describing a solute that frequently dissociates nonidealities, M_{solute} is the molar concentration, R is the ideal gas constant, and T is the temperature expressed in Kelvin. The tested concentrations and van't Hoff indices (2) of MSG and NaCl were identical, and accordingly the corresponding expected fluxes were similar (Eq. (6)).

Fig. 4 shows the measured osmotic pressure of MSG and NaCl solution for tested concentration range. Osmolarity increased linearly as the concentration of MSG and NaCl increased in the experimental concentration range. Measured value for MSG and NaCl were almost identical. The relatively lower flux with MSG compared to NaCl can be explained by the lower diffusivity, which results in severer concentration polarization (McCutcheon *et al.* 2006, Zhao *et al.* 2011).

Solution-diffusion model for FO process derives the following equations for water and salt fluxes.

$$J_w = A \left\{ \frac{\pi_D \exp\left(-\frac{J_w S}{D}\right) - \pi_F \exp\left(\frac{J_w}{k}\right)}{1 + \frac{B}{J_w} \left[\exp\left(\frac{J_w}{k}\right) - \exp\left(-\frac{J_w S}{D}\right) \right]} \right\} \quad (7)$$

$$J_s = B \left\{ \frac{C_D \exp\left(-\frac{J_w S}{D}\right) - C_F \exp\left(\frac{J_w}{k}\right)}{1 + \frac{B}{J_w} \left[\exp\left(\frac{J_w}{k}\right) - \exp\left(-\frac{J_w S}{D}\right) \right]} \right\} \quad (8)$$

For comparison, water and salt permeability coefficients, A and B , and structure parameter (S) were determined numerically by using the method proposed by Tiraferri *et al.* (2013). Water permeability coefficient (A) and membrane structure parameter (S) are regarded as intrinsic values for a specific membrane. With NaCl as the reference draw solute at the well-reported concentration range (0.5 – 3 M), A , B and S were obtained as 0.712 L/m²h bar⁻¹ and 0.441 L/m²h, and 677 μm, respectively. The coefficients of determination (R^2) for J_w and J_s were 0.996

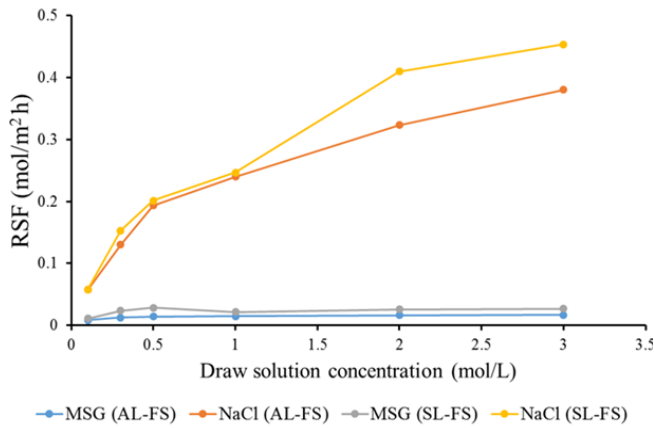


Fig. 5 RSFs of the FO processes using MSG and NaCl as draw solutes with HTI CTA membrane

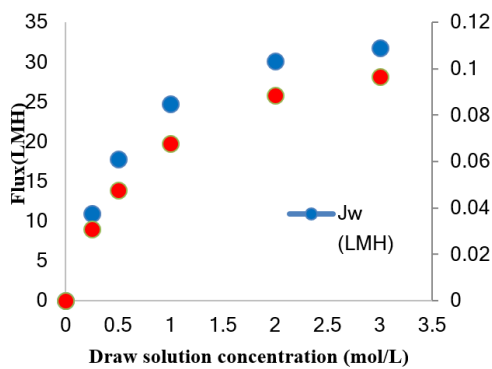


Fig. 6 Water flux and RSF of the FO processes with mLBL FO membrane using MSG as draw solutes

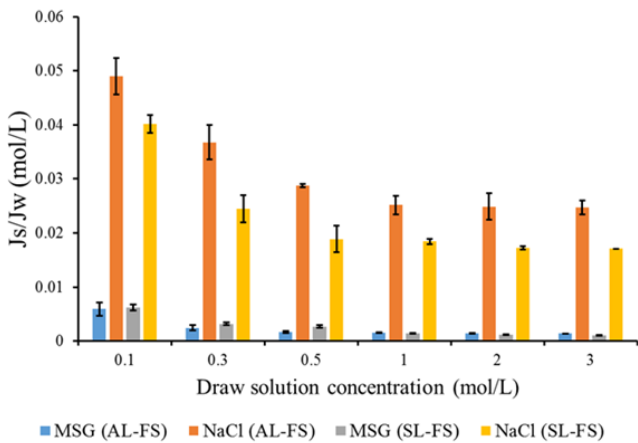


Fig. 7 J_s/J_w ratios of the FO processes using MSG and NaCl as draw solutes with HTI CTA membrane

and 0.987, respectively. These values are similar to those in FO experiments with the same DS (NaCl) and membrane (Tiraferri *et al.* 2013, D’Haese *et al.* 2017).

Fig. 5 shows the RSFs of the FO processes with CTA membrane in the AL–FS and SL–FS modes. For both draw solute, RSF increased with increasing DS concentration (Phillip *et al.* 2010). In the SL–FS mode, the RSF of the FO processes using the MSG solutions (3M) was 0.027 mol/m²h, while in the AL–FS mode the RSF was 0.017 mol/m²h. In the SL–FS mode, the RSF of the FO processes

using the NaCl solutions (3M) was 0.45 mol/m²h, while that in the AL–FS mode was 0.38 mol/m²h. The RSFs of the FO processes using the both draw solutions at different concentrations in the AL–FS mode were lower than those in the SL–FS mode.

Regardless of the driving mode, the RSF of the FO process using MSG as a draw solute was significantly lower than that of the process using NaCl. Low RSF is critical for ideal draw solute to fulfill the requirements for FO process design (Ge *et al.* 2013). High molecular weight and low diffusivity of MSG compared to NaCl can explain the difference.

With the structure parameter (S) value, diffusivity (D), mass transfer coefficient (k) and experimental data for water and salt fluxes (J_w and J_s), salt permeability (B) for MSG can be calculated from Eq. (8). Diffusivity of MSG referred the table 1. ECP is negligible (i.e., $\exp(J_w/k) = 1$). For the concentration range of 1 – 3M, B value was obtained as 0.136 – 0.086 L/m²h. As expected, the values are relatively lower than that of NaCl.

Fig. 6 shows the FO test results with mLBL membrane in the AL–FS mode. Water flux increased almost 3 times compared to the results with HTI CTA membrane, however, RSF also increased.

Maximum water flux (J_w) through the FO membrane with minimum reverse permeation of solute (J_s) is critical for system efficiency. Much lower J_s/J_w value was obtained with MSG than NaCl for the same concentration (Fig. 7), while similar water flux was obtained.

In the case of NaCl, the J_w value in SL–FS mode was about twice as large as that in AL–FS mode, and the value of J_s in SL–FS mode was also relatively larger than that in AL–FS mode, but it was not up to twice. Therefore, The J_s/J_w ratios showed a larger value in AL–FS mode than in SL–FS mode. However, in the case of MSG, the difference in J_s/J_w value depending on mode was not noticeable.

The J_s/J_w ratios of the FO processes using the MSG solution at 3M were 0.0011mol/L and 0.0014mol/L in the In the SL–FS mode and AL–FS mode, respectively. In the SL–FS mode, the J_s/J_w ratio of the FO processes using the NaCl solution (3M) was 0.017 mol/L, while that in the AL–FS mode was 0.025 mol/L. J_s/J_w is the loss of DS into the feed solution over unit water permeation through membrane. J_s/J_w decreased with the DS concentration in all cases with NaCl and MSG.

If the A, B, and S values are intrinsic to a specific membrane and are not affected by the salt concentration, J_s/J_w must remain constant as the salt concentration changes. When salt concentration is dilute, osmotic pressure becomes proportional to salt concentration, and ICP, that is, $\exp(-J_w K)$ is a relatively small value compared to J_w , then J_s/J_w can be expressed by the following simple equation (Phillip *et al.* 2010).

$$\frac{J_s}{J_w} = \frac{B}{A i R T} \quad (9)$$

J_s/J_w is determined solely by the characteristics of the active layer of the membrane and the characteristics of draw solute, regardless of the support layer structure parameter and DS concentration. However, studies have reported that

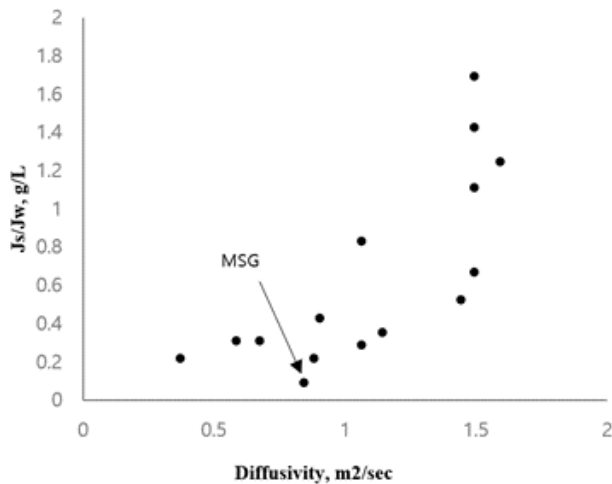


Fig. 8 Diffusivity of draw solutes versus J_s/J_w

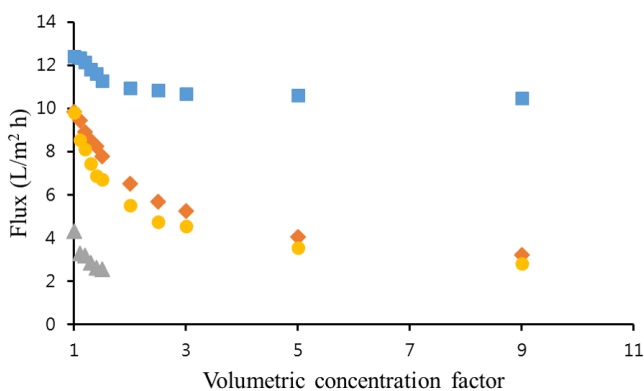


Fig. 9 Flux change during sewage thickening by FO with MSG as DS (■: Blank-run with DI water as feed solution, ◆: Run-1 for sewage thickening, ▲: Run-2 after DS replacement, ●: Run-3 after membrane flushing and DS replacement)

J_s/J_w is affected by DSs and their concentration also (Hau *et al.* 2014, Linares *et al.* 2013). D'Haese *et al.* (2017) analyzed the effect of the concentration of draw solutes on the permeability of water and salt to the membrane in FO, and observed that the values vary according to the concentration of draw solute.

J_w and J_s increased with increasing DS (Figs. 3 and 5), but the ratio was not constant, and J_s/J_w tended to be high at relatively low concentration (Fig. 7). On the other hand, FO test with mLBL membrane in the tested concentration range of MSG, calculated J_s/J_w value were slightly higher than that with HTI CTA, and relatively constant.

From the results, the dependence of J_w , J_s and J_s/J_w on DS concentration suggests careful selection of applicable concentrations of MSG as DS. That is, the water permeation flux is not linearly proportional to the DS concentration, and the salt leakage rate depends on the FO membrane and DS concentration. On the other hand, DS recovery by NF at high concentrations is practically difficult due to high energy requirements and leakage of salt. Therefore, the DS concentration affects the system economics.

For the concentration and reclamation of sewage,

several draw solutes have been proposed (Lutchmiah *et al.* 2014, Ansari *et al.* 2015). Fig. 8 shows J_s/J_w versus diffusivity of the suggested draw solutes using the same CTA FO membrane from HTI. Plot shows that J_s/J_w is related to the diffusivity of DS.

3.2 Application of MSG to sewage thickening

The sewage collected from the primary sedimentation basin of municipal wastewater treatment plant was thickened up to 9 times by FO mode using MSG as draw solute. During the process, J_w was decreased due to fouling. (Fig. 9). The blank-run with DI water for feed was used as the reference for DS dilution by the permeated water during the thickening. In blank-run, the final water flux was 10.5 L/m²h, which was 15.6% lower than the initial flux. Although fouling was not generated in the active layer, the water flux decreased as purified water crossed the membrane from the feed to the draw side and diluted the draw solution from the feed to the draw side and diluted the draw solution from 1M to 0.53M, decreasing the osmotic pressure of the draw solution. In run-1 of sewage thickening, the initial water flux was 9.8 L/m²h, which was 20.8% lower than its initial value in blank-run. The difference was considered due to the irreversible fouling. The final water flux in run-1 was 3.2 L/m²h, which was 67.5% lower than the initial flux of run-1. The foulants in the sewage accumulated on the active layer and prevented the purified water from passing from the feed side to the draw side. After run-1, diluted draw solution was replaced with fresh MSG solution and membrane was reused in run-2. Water flux was slightly increased because of the restored water-drawing capacity by replaced draw solution. However, water flux rapidly decreased due to membrane fouling and sewage thickening could not proceed further. The initial water flux of run-2 was 4.3 L/m²h, while the final water flux was 2.5 L/m²h, when the sewage was thickened 1.5 times. After washing of the active layer and replacement of the draw solution, water flux was recovered. The initial water flux of run-3 was identical to the initial value in run-1. Therefore, the fouling through the run-1 and run-2 was reversible and the foulants were easily removed by water flushing.

These results demonstrate that physical flushing can efficiently remove foulants from the active layer of the FO membrane. It is suggested that with increased cross-flow velocity, reversible fouling on the surface of active layer can be retarded (Kim *et al.* 2016). However, the reused membrane after the physical flushing was less effective than a fresh membrane owing to the irreversible fouling of the active layer. Osmotic backwashing and chemical cleaning can recover the irreversible fouling (Holloway *et al.* 2007, Mi *et al.* 2010).

3.3 Draw solute recovery by NF

By nanofiltration MSG was efficiently recovered. The rejection of MSG was higher compared to those of NaCl as expected. Fig. 10 shows the solute rejections of the NF processes of MSG and NaCl solutions with NE4040-90. The rejections of MSG for solutions of 0.1, 0.15, 0.2, 0.25,

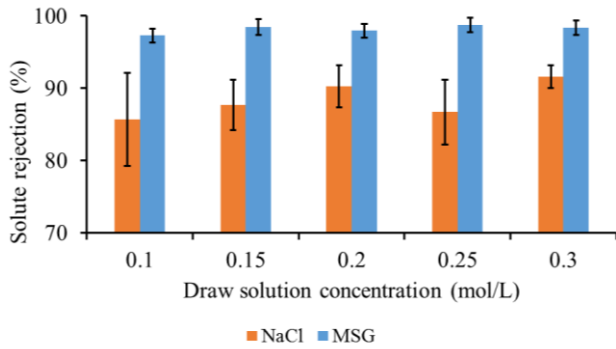


Fig. 10 DS rejections by NE4040-90 at 10 bar

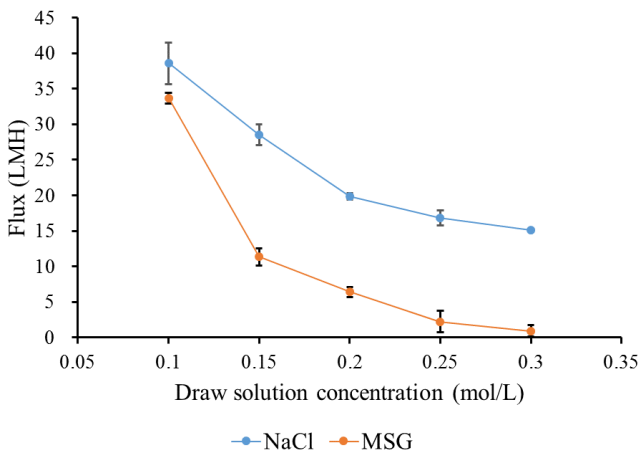


Fig. 11 DS concentration vs Water flux of the NF with NE4040-90 at 10 bar

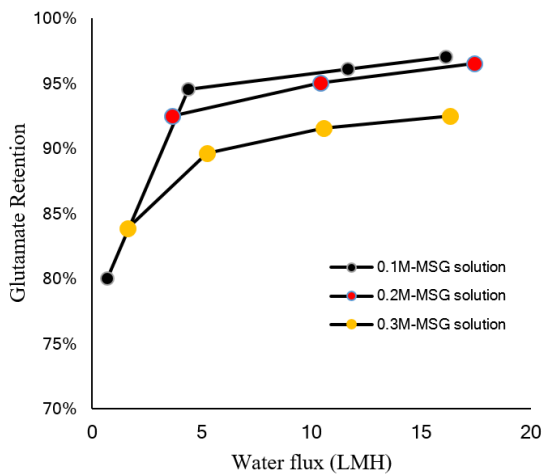


Fig. 12 Glutamate retention by NF4040 membrane with varied MSG concentration

and 0.3 M were 97.3, 98.5, 98.0, 98.8, and 98.3%, respectively. On the other hand, the rejections of NaCl solutions (0.1, 0.15, 0.2, 0.25, and 0.3 M) were 85.7, 87.8, 90.2, 86.7, and 91.6%, respectively. According to the results, the purity of water produced using the NF process in the MSG solution is quite high ($\geq 97\%$).

Separation of solute by NE4040-90 is influenced by the size and charge of the solute. MWCO of NF membrane was 210. Therefore, the rejection is not apparently by

size-exclusion. Steric hindrance and charge repulsion were suggested to explain the rejection. Transmission of solutes through NF membrane is governed by diffusion and migration. Concentration and electrical potential gradient give molecular diffusion and pressure difference drive convective migration of solutes. This process has been described by Nernst-plank equation. (Mohammad *et al.* 2015). When the membrane has a charge, the effect of rejection by Donnan equilibrium is important. The negatively charged NF membrane used in this experiments repulse the negatively charged co-ions. Since the electro neutrality of the feed solution must be maintained, the counter ion (Na^+) is rejected to the same extent.

The results in Fig. 10 agree well with the rejection values for NaCl provided by the manufacturer. The pH of MSG solutions were near neutral value. At this pH, dissociated glutamate has a net charge value of -1. However, it is a divalent anion having -2 for z- and +1 for z+ values, therefore it undergoes membrane repulsion stronger than Cl^- and relatively high rejection. (Martin-Orue *et al.* 1998).

Fig. 11 shows the initial water fluxes of the NF processes with NE4040-90 membrane for DS solute recovery at 10 bar. The water fluxes for the MSG solutions (initial concentration: 0.1, 0.15, 0.2, 0.25, and 0.3 M) were 33.6, 11.4, 6.4, 2.25, and 0.9 $\text{L}/\text{m}^2 \text{h}$, respectively. The water fluxes of the NF processes using the NaCl solutions (0.1, 0.15, 0.2, 0.25, and 0.3 M) were 38.6, 28.5, 19.8, 16.8, and 15.1 $\text{L}/\text{m}^2 \text{h}$, respectively. When the MSG concentration was over 0.3 M, the water flux was almost zero. To increase the water permeation, applied pressure or membrane surface area should be increased with energy and installation cost.

These results show that DS concentration should be carefully decided in the FO–NF hybrid process. For FO, increased DS concentration will give more water permeation, while J_s will also be increased. However, at high concentration incremental J_w will be decreased due to ICP. Low J_s/J_w is beneficial for operational cost management, which depends upon the choice of FO membrane, DS and DS concentration. High concentrations of the DS reduced the flux in the NF, while low concentrations of the DS reduced the flux in the FO. The overall system performance will be influenced by FO fouling control, DS loss, and NF operation efficiency.

Pressure difference and feed concentration influence the water permeation flux, and increased initial concentration of ionic feed solution can change the retention in NF filtration. Fig. 12 shows the change of glutamate retention of NF4040 membrane with applied pressure and MSG concentration varied. Increase in water flux gives high glutamate retention, while increase in initial MSG concentration lowered the retention.

Glutamate and NF membrane have charges, which is influenced by solution chemistry. Fig. 13 shows the glutamate retention by NF using NF40404 membrane at acidic, neutral and basic pH. Acidic and basic MSG solution was obtained by adding NaOH and HCl to MSG solution, while 0.3M MSG solution has pH value near neutral at 7.6. At both acidic and basic pH, glutamate retention was decreased compared to neutral pH.

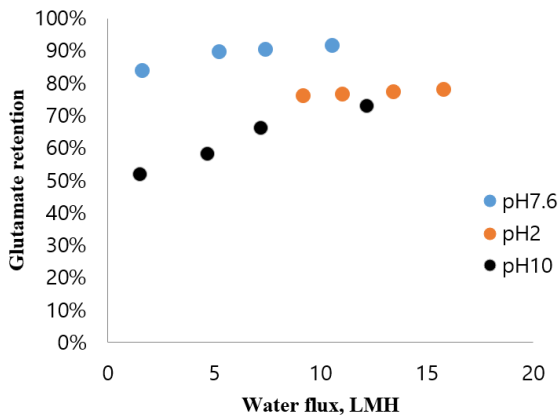


Fig. 13 Glutamate retention by NF4040 membrane with varied pH

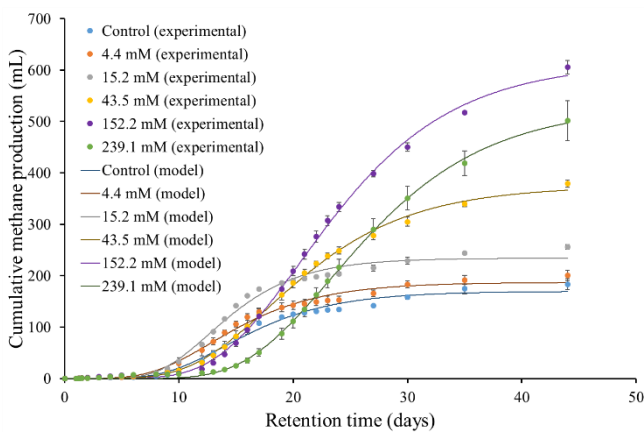


Fig. 14 Cumulative methane productions (dots) and predicted methane productions fitted by the Gompertz model (solid curves)

It has been known that the mechanism of salt retention by NF is governed by steric exclusion and Donnan equilibrium. (Yaroshchuk *et al.* 2019). Neutralization of the surface charge of the membrane by the added counter ion (cation) can also affect the rejection of co-ions. NF rejection of multi ionic solutions is complicated process.

The net charge of Zwitteric glutamate ion changes with pH. The surface of NF4040 membrane has negative charge, providing an electrical repulsion to the negative ions, however at low pH the surface potential of the NF membrane shifts to a positive value, which will influence the retention of glutamate.

3.4 Evaluation of the inhibitory effect of MSG on the FO-based wastewater treatment process

The ATA was carried out to evaluate the inhibitory effects of MSG on the methane production (Owen *et al.* 1797, Gartiser *et al.* 2007). The cumulative methane production was periodically monitored in all batch runs (Fig. 14). Based on the results, the methane production potential, maximum methane production rate, and lag period were determined using a modified Gompertz model (Zwietering *et al.* 1990, Lay *et al.* 1998) (Fig. 14).

Fig. 14 shows the methane production patterns under

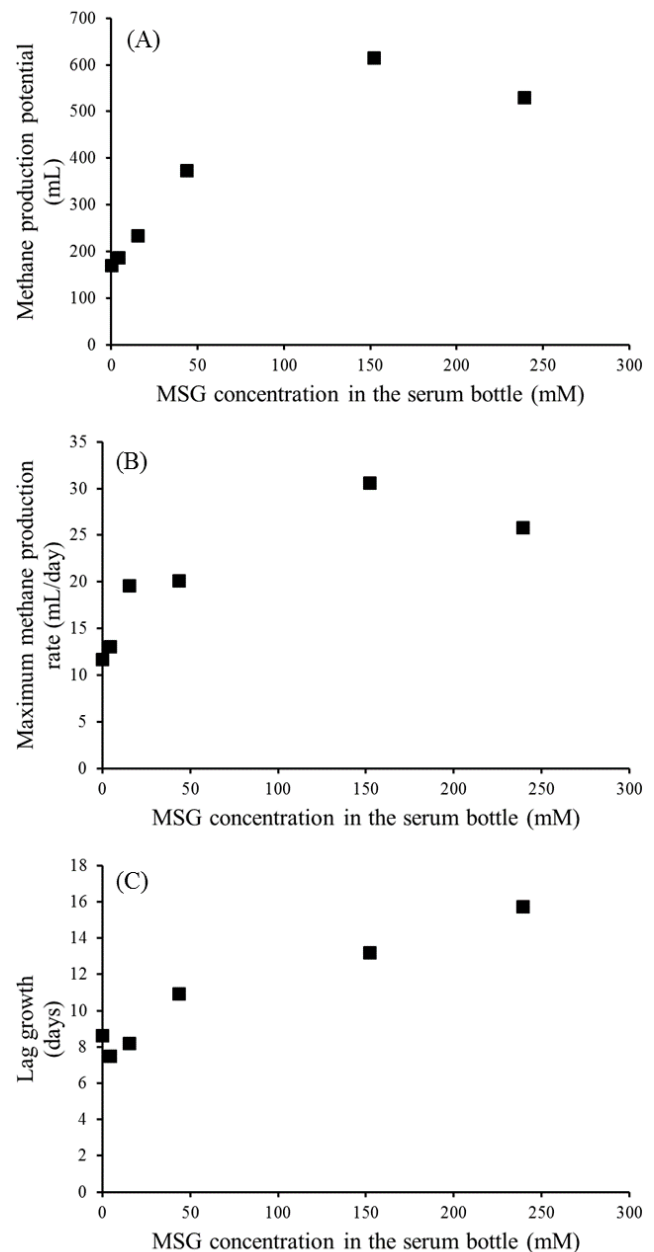


Fig. 15 (A) Methane production potentials, (B) maximum methane production rates, and (C) lag periods based on the modified Gompertz model

each experimental condition. The methane production depended on the MSG concentration. At MSG concentrations of 0, 4.4, and 15.2 mM, the methane gas generation lasted almost eight days, corresponding to the highest rate among those of the experimental sets. At MSG concentrations of 43.5, 152.1, and 238.1 mM, the methane production began after 11, 13, and 16 days, respectively. At MSG concentrations of 4.4, 15.2, 43.5, 152.2, and 239.1 mM, 200.9, 255.7, 379.0, 605.5, and 501.9 mL of methane were produced, respectively. In the control run, 183.6 mL of methane were produced, indicating that the methane production was higher than that of the control run at all of the experimental conditions. Therefore, the methane production and the time at which its generation began

increased with the MSG concentration. The modified Gompertz model was used to assess the toxicity of MSG in the methane production (Fig. 15).

Figs. 15(A) and 15(B) show the calculated results for the methane production potentials and maximum methane production rates. At MSG concentrations of 0, 4.4, 15.2, 43.5, 152.2, and 239.1 mM, the calculated methane production potentials were 169.6, 187.0, 234.2, 374.4, 614.9, and 530.4 mM, while the calculated maximum methane production rates were 11.7, 13.0, 19.6, 20.1, 30.6, and 25.8 mL/day, respectively. The methane production potentials and maximum methane production rates gradually increased with the MSG concentration up to 239.1 mM. The results indicate that the glutamate of MSG was converted to methane during the batch operation [18, 30]. However, a different trend was observed for the lag period compared with those of the methane production potential and maximum methane production rate (Fig. 11->14 (C)), which could be due to the inhibitory effect of sodium. In this study, at MSG concentrations of 43.5, 152.2, and 239.1 mM (sodium ion concentrations: 1000, 3500, and 5500 mg/L), the lag periods increased to 126.6, 152.8, and 182.2% of that of the control run, respectively. Sodium ion concentrations of 3500–5500 mg/L lead to a moderate inhibitory effect on methanogenic archaea (Chen *et al.* 2008, Kugelman *et al.* 1964). Therefore, the increased sodium ion concentration inhibited the microbial activity, which could eventually extend the lag period. It is worth noting that at MSG concentrations of 4.4 and 15.2 mM (sodium ion concentrations: 100 and 350 mg/L), the lag periods decreased to 87 and 95% of that of the control run, respectively. According to the previous studies, sodium ion concentrations of 100–200 mg/L can promote the growth of mesophilic anaerobes (Chen *et al.* 2008, Kugelman *et al.* 1964). It has been also suggested that a sodium ion concentration of 350 mg/L is optimal for the growth of mesophilic methanogens (Chen *et al.* 2008, Patel *et al.* 1977). Therefore, the ATA results show that the methane production potential and maximum methane production rate were increased at an MSG concentration \leq 15.2 mM, compared to those in the control run, but the lag period was decreased. This suggests that MSG originated from the RSF can be recovered as methane gas without significant inhibition through the AD.

4. Conclusions

In this study, the efficiency of MSG as DS for sewage thickening using FO, recovery of MSG using NF, and inhibitory effect of MSG on AD were investigated. The following conclusions can be summarized:

- MSG has a low J_s/J_w value, confirming its practical potential as a DS for application to the FO process.
- Using the FO process with MSG as DS, the sewage (primary wastewater) could be thickened more than nine times and the water flux was recovered by 87.5% using physical flushing.
- MSG can be efficiently recycled with a high recovery rate by NF.

- ATA tests show that MSG solution was not generated inhibition at below 15.2 mM, and methane production was not decreased at below 152.2 mM. Considering that the amount of MSG passing through the FO membrane when producing 1 L of water was about 1.1 to 1.4 mM, it is considered possible to apply the concentrated sewage using FO process to the AD process.

Acknowledgments

This research was financially supported by the Korea Institute of Science and Technology (Project Codes: 2E26251, 2E29660). This study was also supported by the KU-KIST Graduate School Project.

References

- Achilli, A., Cath, T.Y. and Childress, A.E. (2009), "Power generation with pressure retarded osmosis: An experimental and theoretical investigation", *J. Membr. Sci.*, **343**(1), 42-52. <https://doi.org/10.1016/j.memsci.2009.07.006>.
- Achilli, A., Cath, T.Y. and Childress, A.E. (2010), "Selection of inorganic-based draw solutions for forward osmosis applications", *J. Membr. Sci.*, **364**(1), 233-241. <https://doi.org/10.1016/j.memsci.2010.08.010>.
- Ansari, A.J., Hai, F.I., Guo, W., Ngo, H.H., Price, W.E. and Nghiem, L.D. (2015), "Selection of forward osmosis draw solutes for subsequent integration with anaerobic treatment to facilitate resource recovery from wastewater", *Bioresource Technol.*, **191**, 30-36. <https://doi.org/10.1016/j.biortech.2015.04.119>.
- Batstone, D.J., Hülsen, T., Mehta, C.M. and Keller, J. (2015), "Platforms for energy and nutrient recovery from domestic wastewater: A review", *Chemosphere*, **140**, 2-11. <https://doi.org/10.1016/j.chemosphere.2014.10.021>.
- Bowden, K.S., Achilli, A. and Childress, A.E. (2012), "Organic ionic salt draw solutions for osmotic membrane bioreactors", *Bioresource Technol.*, **122**, 207-216. <https://doi.org/10.1016/j.biortech.2012.06.026>.
- Cath, T.Y., Childress, A.E. and Elimelech, M. (2006), "Forward osmosis: Principles, applications, and recent developments", *J. Membr. Sci.*, **281**(1-2), 70-87. <https://doi.org/10.1016/j.memsci.2006.05.048>.
- Chen, L., Gu, Y., Cao, C., Zhang, J., Ng, J.W. and Tang, C. (2014), "Performance of a submerged anaerobic membrane bioreactor with forward osmosis membrane for low-strength wastewater treatment", *Water Res.*, **50**, 114-123. <https://doi.org/10.1016/j.watres.2013.12.009>.
- Chen, Y., Cheng, J.J. and Creamer, K.S. (2008), "Inhibition of anaerobic digestion process: A review", *Bioresource Technol.*, **99**(10), 4044-4064. <https://doi.org/10.1016/j.biortech.2007.01.057>.
- D'Haese, A.K.H., Motsa, M.M., Meeren, P.V.D. and Verliefde, A.R.D. (2017), "A refined draw solute flux model in forward osmosis: Theoretical considerations and experimental validation", *J. Membr. Sci.*, **522**, 316-331. <https://doi.org/10.1016/j.memsci.2016.08.053>.
- Gartiser, S., Urich, E., Alexy, R. and Kummerer, K. (2007), "Anaerobic inhibition and biodegradation of antibiotics in ISO test schemes", *Chemosphere*, **66**(10), 1839-1848. <https://doi.org/10.1016/j.chemosphere.2006.08.040>.
- Ge, Q., Su, J., Amy, G.L. and Chung, T.S. (2012), "Exploration of polyelectrolytes as draw solutes in forward osmosis processes", *Water Res.*, **46**(4), 1318-1326.

- <https://doi.org/10.1016/j.watres.2011.12.043>.
- Ge, Q.C., Ling, M.M. and Chung, T.S. (2013), "Draw solutions for forward osmosis processes: Developments, challenges, and prospects for the future", *J. Membr. Sci.*, **442**, 225-237. <https://doi.org/10.1016/j.memsci.2013.03.046>.
- Ghadiri, L., Bozorg, A. and Shakeri, A. (2019), "Electrospun polyamide thin film composite forward osmosis membrane: Influencing factors affecting structural parameter", *Membr. Water Treat.*, **10**(6), 417-429. <https://doi.org/10.12989/mwt.2019.10.6.417>.
- Hau, N.T., Chen, S.S., Nguyen, N.C., Huang, K.Z., Ngo, H.H. and Guo, W. (2014), "Exploration of EDTA sodium salt as novel draw solution in forward osmosis process for dewatering of high nutrient sludge", *J. Membr. Sci.*, **455**, 305-311. <https://doi.org/10.1016/j.memsci.2013.12.068>.
- Holloway, R.W., Childress, A.E., Dennett, K.E. and Cath, T.Y. (2007), "Forward osmosis for concentration of anaerobic digester centrate", *Water Res.*, **41**(17), 4005-4014. <https://doi.org/10.1016/j.watres.2007.05.054>.
- ISO (2003), "Water quality—Determination of inhibition of gas production of anaerobic bacteria. Part 1: General test", ISO 13641-1:2003.
- Jiang, S.K., Zhang, G.M., Yan, L. and Wu, Y. (2018), "Treatment of natural rubber wastewater by membrane technologies for water reuse", *Membr. Water Treat.*, **9**(1), 17-21. <https://doi.org/10.12989/mwt.2018.9.1.017>.
- Kim, B., Gwak, G. and Hong, S. (2017), "Review on methodology for determining forward osmosis (FO) membrane characteristics: Water permeability (A), solute permeability (B), and structural parameter (S)", *Desalination*, **422**, 5-16. <https://doi.org/10.1016/j.desal.2017.08.006>.
- Kim, D.I., Kim, J. and Hong, S. (2016), "Changing membrane orientation in pressure retarded osmosis for sustainable power generation with low fouling", *Desalination*, **389**, 197-206. <https://doi.org/10.1016/j.desal.2016.01.008>.
- Kravath, R.E. and Davis, J.A. (1975), "Desalination of sea-water by direct osmosis", *Desalination*, **16**(2), 151-155. [https://doi.org/10.1016/S0011-9164\(00\)82089-5](https://doi.org/10.1016/S0011-9164(00)82089-5).
- Kugelman, I.J. and McCarty, P.L. (1965), "Cation toxicity and stimulation in anaerobic waste treatment", *J. Water Pollut. Control. Fed.*, 97-116.
- Kumar, R. and Pal, P. (2015), "A novel forward osmosis-nano filtration integrated system for coke-oven wastewater reclamation", *Chem. Eng. Res. Des.*, **100**, 542-553. <https://doi.org/10.1016/j.cherd.2015.05.012>.
- Kwon, S.B., Lee, J.S., Kwon, S.J., Yun, S.T., Lee, S. and Lee, J.H. (2015) "Molecular layer-by-layer assembled forward osmosis membranes", *J. Membr. Sci.* **488**, 111-120. <https://doi.org/10.1016/j.memsci.2015.04.015>.
- Lay, J.J., Li, Y.Y. and Noike, T. (1998), "Mathematical model for methane production from landfill bioreactor", *J. Environ. Eng.*, **124**(8), 730-736.
- Lee, S., Quyet, N., Lee, E., Kim, S., Lee, S., Jung, Y.D., Choi, S.H. and Cho, J. (2008), "Efficient removals of tris(2-chloroethyl) phosphate (TCEP) and perchlorate using NF membrane filtrations", *Desalination*, **221**(1), 234-237. <https://doi.org/10.1016/j.desal.2007.02.054>.
- Li, D., Zhang, X., Yao, J., Simon, G.P. and Wang, H. (2011), "Stimuli-responsive polymer hydrogels as a new class of draw agent for forward osmosis desalination", *Chem. Commun.*, **47**(6), 1710-1712. <https://doi.org/10.1039/C0CC04701E>.
- Ling, M.M. and Chung, T.S. (2011), "Novel dual-stage FO system for sustainable protein enrichment using nanoparticles as intermediate draw solutes", *J. Membr. Sci.*, **372**(1), 201-209. <https://doi.org/10.1016/j.memsci.2011.02.003>.
- Liu, C., Li, H., Zhang, Y., Si, D. and Chen, Q. (2016), "Evolution of microbial community along with increasing solid concentration during high-solids anaerobic digestion of sewage sludge", *Bioresour. Technol.*, **216**, 87-94. <https://doi.org/10.1016/j.biortech.2016.05.048>.
- Lutchmiah, K., Lauber, L., Roest, K., Harmsen, D.J.H., Post, J.W., Rietveld, L.C., Van Lier, J.B. and Cornelissen, E.R. (2014), "Zwitterions as alternative draw solutions in forward osmosis for application in wastewater reclamation", *J. Membr. Sci.*, **460**, 82-90. <https://doi.org/10.1016/j.memsci.2014.02.032>.
- Martin Orue, C., Bouhallab, S. and Garem, A. (1998), "Nanofiltration of amino acid and peptide solutions: mechanisms of separation", *J. Membr. Sci.*, **142**(2), 225-233. [https://doi.org/10.1016/S0376-7388\(97\)00325-6](https://doi.org/10.1016/S0376-7388(97)00325-6).
- McCutcheon, J.R. and Elimelech, M. (2006), "Influence of concentrate and dilute internal concentration polarization on flux behavior in forward osmosis", *J. Membr. Sci.*, **284**(1), 237-247. <https://doi.org/10.1016/j.memsci.2006.07.049>.
- McCutcheon, J.R., McGinnis, R.L. and Elimelech, M. (2006), "Desalination by ammonia-carbon dioxide forward osmosis: Influence of draw and feed solution concentrations on process performance", *J. Membr. Sci.*, **278**(1-2), 114-123. <https://doi.org/10.1016/j.memsci.2005.10.048>.
- Mi, B. and Elimelech, M. (2010), "Organic fouling of forward osmosis membranes: Fouling reversibility and cleaning without chemical reagents", *J. Membr. Sci.*, **348**(1), 337-345. <https://doi.org/10.1016/j.memsci.2009.11.021>.
- Mohammad, A.W., Teow, Y.H., Ang, W.L., Chung, Y.T., Oatley-Radcliffe, D.L. and Hilal, N. (2015), "Nanofiltration membranes review: Recent advances and future prospects", *Desalination*, **356**, 226-254. <https://doi.org/10.1016/j.desal.2014.10.043>.
- Owen, W.F., Stuckey, D.C., Healy, J.B., Young, L.Y. and McCarty, P.L. (1979), "Bioassay for monitoring biochemical methane potential and anaerobic toxicity", *Water Res.*, **13**(6), 485-492.
- Patel, G.B. and Roth, L.A. (1977), "Effect of sodium chloride on growth and methane production of methanogens", *Can. J. Microbiol.*, **23**(7), 893-897. <https://doi.org/10.1139/m77-131>.
- Phillip, W.A., Yong, J.S. and Elimelech, M. (2010), "Reverse draw solute permeation in forward osmosis: Modeling and experiments", *Environ. Sci. Technol.*, **44**(13), 5170-5176. <https://doi.org/10.1021/es100901n>.
- Ribeiro, A.C.F., Rodrigo, M.M., Barros, M.C.F., Verissimo, L.M.P., Romero, C., Valente, A.J.M. and Estes, M.A. (2014), "Mutual diffusion coefficients of L-glutamic acid and monosodium L-glutamate in aqueous solutions at T=298.15K", *J. Chem. Thermodyn.*, **74**, 133-137. <https://doi.org/10.1016/j.jct.2014.01.017>.
- Tiraferri, A., Yip, N.Y., Straub, A.P., Castrillon, S.R.V. and Elimelech, M. (2013), "A method for the simultaneous determination of transport and structural parameters of forward osmosis membranes", *J. Membr. Sci.*, **444**, 523-538. <https://doi.org/10.1016/j.memsci.2013.05.023>.
- Linares, R.V., Li, Z., Abu Ghdaib, M., Wei, C.H., Amy, G. and Vrouwenvelder, J.S. (2013), "Water harvesting from municipal wastewater via osmotic gradient: An evaluation of process performance", *J. Membr. Sci.*, **447**, 50-56. <https://doi.org/10.1016/j.memsci.2013.07.018>.
- Xue, W., Tobino, T., Nakajima, F. and Yamamoto, K. (2015), "Seawater-driven forward osmosis for enriching nitrogen and phosphorus in treated municipal wastewater: Effect of membrane properties and feed solution chemistry", *Water Res.*, **69**, 120-130. <https://doi.org/10.1016/j.watres.2014.11.007>.
- Yaroshchuk A., Bruening M.L. and Zholkovskiy E. (2019), "Modelling nanofiltration of electrolyte solutions", *Adv. Colloid Interfac.*, **268**, 39-63. <https://doi.org/10.1016/j.cis.2019.03.004>.
- Yong, J.S., Phillip, W.A. and Elimelech, M. (2012), "Coupled reverse draw solute permeation and water flux in forward osmosis with neutral draw solutes", *J. Membr. Sci.*, **392**, 9-17.

<https://doi.org/10.1016/j.memsci.2011.11.020>.

Zhao, S. and Zou, L. (2011), “Relating solution physicochemical properties to internal concentration polarization in forward osmosis”, *J. Membr. Sci.*, **379**(1), 459-467.

<https://doi.org/10.1016/j.memsci.2011.06.021>.

Zwietering, M.H., Jongenburger, I., Rombouts, F.M. and Van't Riet, K. (1990), “Modeling of the bacterial growth curve”, *Appl. Environ. Microbiol.*, **56**(6), 1875-1881.

<https://doi.org/10.1128/aem.56.6.1875-1881.1990>.

SL